

# Research on Multidisciplinary Analysis Tool based on Parametric Model of Hypersonic Morphing Waverider

Yanbin Liu<sup>1</sup>, Liangqiang Zhou<sup>2,\*</sup> and Yuping Lu<sup>1</sup>

<sup>1</sup> College of Astronautics, Nanjing University of Aeronautics and Astronautics, 29 Yudao St., Nanjing 210016, China

<sup>2</sup> College of Sciences, Nanjing University of Aeronautics and Astronautics, 29 Yudao St., Nanjing 210016, China.

Received: 14 Nov. 2014, Revised: 14 Feb. 2015, Accepted: 15 Feb. 2015

Published online: 1 Jul. 2015

**Abstract:** Hypersonic waverider design is a challenging task due to the strong coupling relations between the integrated system and flight performance, thus the development of the multidisciplinary analysis tool is necessary to implement the complex design demands. In this paper, the multidisciplinary design methods are studied to construct the control-related analysis tool for hypersonic morphing waverider. First, the realization process of the integrated design is provided for the morphing waverider in terms of the hypersonic flight characteristics. Then the nonlinear parametric model of hypersonic morphing vehicle is built with the consideration of the shape parameterization and force estimation. Afterwards, the multidisciplinary analysis platform is implemented in relation to the control-related requirements. Finally, a simulation example is given to verify the feasibility of the presented methods for hypersonic morphing waverider.

**Keywords:** Hypersonic morphing waverider, multidisciplinary analysis tool, nonlinear dynamic model, control integrated design.

## 1 Introduction

A prominent feature of the hypersonic waverider manifests in the strong coupling relationship among the various components, such as the aerodynamic shape, the propulsive performance and the control action [1]. Correspondingly, the flight system must be highly integrated to achieve the excellent properties, but such design ideas are challenging due to the significant differences in comparison with the traditional design procedure [2]. As a result, the application of the multidisciplinary tool is critical to realize the waveriding flight goal, and this work will provide helpful information for the further studies concerning the vehicle structure definition, flight control design and multidisciplinary optimization iteration.

For the analytical demands of the control-related design, the model coefficients of the hypersonic waverider need to be acquired first. However, these modeling data may be difficult to get due to lack of the enough flight tests in the conceptual design stage [3]. On the other hand, the dynamic analysis based on the computational fluid dynamics theories is too complicated to guarantee the efficient and rapid design course [4]. Whereas the

parametric modeling approaches can provide a powerful mean to obtain the model dynamics, and this makes the multidisciplinary analysis and design tactics become possible for hypersonic morphing waverider. More importantly, if the control-integrated design and analysis tool can be developed in advance, the trade-off relationship between the system overall capacity and control ability is found earlier, and this will escape the potential risks due to the unsuitable marriage of the system stability and control response [5]. Also, the parametric model provides an effective way to consider the morphing impact in relation to generalized stability. By the compromise of the control action and morphing effect, the flight performance will ameliorate accordingly such that the optimum system states can constantly keep throughout the given flight envelope.

The parametric modeling methods apply some key parameters to describe the vehicle shape, and then the aerodynamic forces are calculated in line with this designed structure such that the flight performance is relevant to the resulting shape variables. Some parametric design approaches include the quadric curve method [6], B-spline method [7], class-shape-transformation method [8] et al. These parametric methods are used to

\* Corresponding author e-mail: [zlqrex@sina.com](mailto:zlqrex@sina.com)

characterize the vehicle units such as the fuselage, wing and engine, followed that the further works including the shape optimization, dynamic analysis, and control design are conducted. However, the geometrical shape of hypersonic waverider is more complex than that of the conventional vehicle, this mainly reflects in the airframe/engine integration and especial wave-riding configuration. Therefore, the parametric results with respect to the hypersonic waverider tend to be non-analytic functions with the nonlinear and strong coupling characteristics [9]. In this aspect, a parametric design method is proposed to describe the waverider forebody in [10] wherein the energy equation and wedge angle are used to outline the overlooking and side shape in order to decrease the design parameters. Beside that, the control-oriented modeling [11] and adaptive control strategy [12] are developed for hypersonic vehicle in terms of the established parametric model. At the same time, the parametric modeling methods offer the valid means to study the control trade issues with consideration of the multidisciplinary factors [13]. All in all, the combination of the multidisciplinary analysis tool and parametric modeling idea can promote the integrated design of hypersonic waverider, resulting in the improvement of flight performance accordingly.

In this paper, the design methods of the multidisciplinary analysis tool are investigated for hypersonic morphing waverider. There are three aspects of this problem have to be addressed. The first question involves the realization process of the analysis tool that guides the following research. The second problem relates to the parametric modeling with the integration of the multidisciplinary contents. The third aspect deals with the development of the platform tools in accordance with the control constrains. Lastly, a simulation example tests the reliability of the presented methods for hypersonic morphing waverider.

## 2 Realization process of multidisciplinary analysis tool

The typical waverider configuration has the following features: 1) the vehicle forebody is considered as the compression section of the engine, whereas the afterbody is taken into account as the expansion part; 2) the integration of the vehicle fuselage and engine makes the aerodynamic force and thrust interact each other due to the shock wave action, leading to the waveriding performance restricted by the multidisciplinary elements such as aerodynamic, propulsion and control. Thus, the trade-off analysis is crucial for hypersonic waverier to seek the equilibrium relations in the different disciplines [14]. In this study, we select a basic appearance of the waverider as the analysis object, as shown in Figure 1.

For Figure 1, the realization process of the multidisciplinary design based on the parametric model is demonstrated in Figure 2.

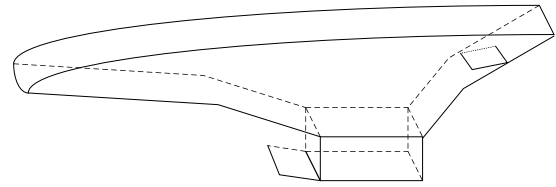


Fig. 1: Typical configuration of hypersonic morphing waverider.

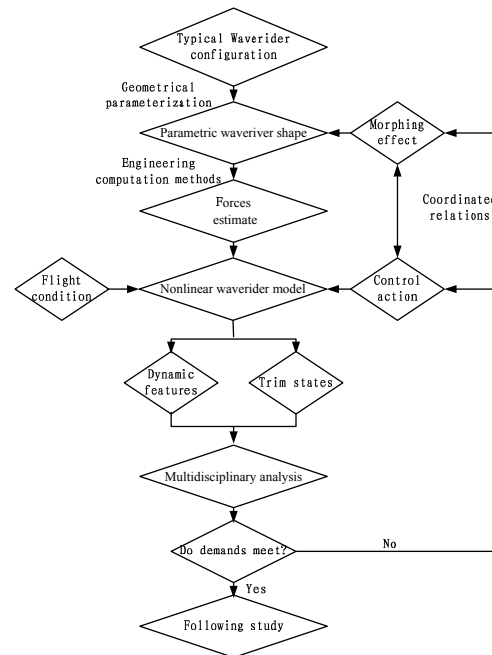


Fig. 2: Realization process of multidisciplinary design.

Figure 2 shows that the proposed realization process of the multidisciplinary design is based on the parametric model involving the multidisciplinary details. In fact, as long as the waverider shape is determined, the according forces are computed by applying the engineering estimation methods. At the same time, the control action and morphing effect are reflected in this parametric model using the fundamental force actions. Furthermore, the analysis tool of hypersonic morphing waverider is developed in terms of the above realization process, thus the iterative design becomes possible. Finally, by the evaluation of the dynamic characteristics and trim states, the trade-off relationship among the different disciplines can be found accordingly for hypersonic morphing waverider, this will be helpful to the follow-up work, such as the robust adaptive control law design and flight trajectory optimization.

### 3 Parametric modeling of hypersonic morphing waverider

The geometrical parameterization of the waverider shape is the basis of the parametric modeling, and how to accurately describe the waveriding motion will decide the intrinsic properties of the built model, thereby affecting the credibility of the multidisciplinary design. In this work, the quadratic curve methods are applied to portray the waverider section, and these curves include circle, ellipse, hyperbola, parabola, etc. By selecting the distinct shape parameters, the combination of the quadratic curves can approach the real vehicle configuration [15]. In particular, the waverider configuration is divided into two kinds of the basic shape: the fuselage class and elevon class. As far as the waverider airframe is concerned, the according profile equations need to be defined first, and then the change tendency along with the body axis is determined accordingly; whereas the elevon shape is assumed as the flat. Correspondingly, the whole waverider shape is constituted by these configurations with regard to the fuselage class and elevon class.

Once the parametric shape of hypersonic waverider is known, the aerodynamic force and propulsive force can be reckoned using the engineering estimate approaches [16]. In this paper, we select the Dahlem-Buck method and Prandtl-Meyer equation to compute the according forces. When the  $i$  th surface panel of hypersonic waverider lies in the windward region, its pressure coefficient  $C_{pi}$  is calculated by the Dahlem-Buck equation, and this is expressed by

$$C_{pi} = C_{pD} \frac{C_{pcone}(Ma \leq 20)}{C_{pcone}(Ma = 20)} \quad (1)$$

$$C_{pD} = \begin{cases} \left[ \frac{1.0}{\sin^{3/4}(4\delta)} + 1 \right] \sin^2 \delta & \delta \leq 22.5^\circ \\ K_b \sin^2 \delta & \delta > 22.5^\circ \end{cases}$$

where

$$\begin{cases} K_b = 2.38 + 0.03792\delta - 0.002521\delta^2 + 0.00004583\delta^3 + 2.917 \times 10^{-7}\delta^4 \\ C_{pcone} = 2e^\xi \sin^2 \theta \\ \xi = 0.18145 - 0.20923\eta + 0.09092\eta^2 + 0.006876\eta^3 - 0.006225\eta^4 - 0.000971\eta^5 \\ \eta = \ln \sqrt{Ma_\infty^2 - 1} \sin \theta \end{cases} \quad (2)$$

where  $\delta$  denotes the airflow impact angle;  $\theta$  represents the surface inclination. The relations among them are given by

$$\begin{cases} \delta = \pi/2 - \cos^{-1} \frac{-\mathbf{n} \cdot \mathbf{V}}{|\mathbf{n}| |\mathbf{V}|}, -90^\circ \leq \delta \leq 90^\circ \\ \theta = \pi/2 - \arccos n_x, -90^\circ \leq \theta \leq 90^\circ \\ \mathbf{V}_\infty = V_x \mathbf{e}_x + V_y \mathbf{e}_y + V_z \mathbf{e}_z \\ \mathbf{n}_i = n_i^x \mathbf{e}_x + n_i^y \mathbf{e}_y + n_i^z \mathbf{e}_z \end{cases} \quad (3)$$

where  $\mathbf{V}_\infty$  is the free stream velocity;  $\mathbf{n}_i$  indicates the normal direction of the  $i$  th surface panel. Therefore, the total pressure coefficients are obtained in the following

forms [17].

$$\begin{cases} C_x = -\sum C_{pi} n_i^x \frac{\Delta S_i}{S_{ref}} \\ C_y = -\sum C_{pi} n_i^y \frac{\Delta S_i}{S_{ref}} \\ C_z = -\sum C_{pi} n_i^z \frac{\Delta S_i}{S_{ref}} \end{cases} \quad (4)$$

where  $\Delta S_i$  and  $S_{ref}$  are the surface element area and vehicle reference area, respectively. Similarly, the moment coefficients are decided by

$$\begin{cases} C_{M_x} = \sum C_{pi} (Z_i n_i^y - Y_i n_i^z) \frac{\Delta S_i}{S_{ref} l_{ref}} \\ C_{M_y} = \sum C_{pi} (X_i n_i^z - Z_i n_i^x) \frac{\Delta S_i}{S_{ref} l_{ref}} \\ C_{M_z} = \sum C_{pi} (Y_i n_i^x - X_i n_i^y) \frac{\Delta S_i}{S_{ref} l_{ref}} \end{cases} \quad (5)$$

where  $\mathbf{r}_i = X_i \mathbf{e}_x + Y_i \mathbf{e}_y + Z_i \mathbf{e}_z$  which denotes the displacement from the  $i$ th surface panel to the vehicle focus, and  $l_{ref}$  is the reference length. In addition, the total forces and moments are computed by

$$\begin{cases} F_x = -\sum p_i n_i^x \Delta S_i \\ F_y = -\sum p_i n_i^y \Delta S_i \\ F_z = -\sum p_i n_i^z \Delta S_i \\ p_i = 0.5 C_{pi} \rho_\infty V_\infty^2 + p_\infty \end{cases} \quad (6)$$

$$\begin{cases} M_x = \sum p_i (Z_i n_i^y - Y_i n_i^z) \Delta S_i \\ M_y = \sum p_i (X_i n_i^z - Z_i n_i^x) \Delta S_i \\ M_z = \sum p_i (Y_i n_i^x - X_i n_i^y) \Delta S_i \end{cases} \quad (7)$$

where  $\rho_\infty$  and  $p_\infty$  represent the density and pressure of free stream, respectively. Thus, the lift and drag of hypersonic waverider are gotten as follows [18].

$$\begin{cases} L = F_x \sin \alpha - F_z \cos \alpha \\ D = -F_x \cos \alpha - F_z \sin \alpha \end{cases} \quad (8)$$

After obtaining these aerodynamic forces, the next work is to estimate the propulsive force required for the model establishment. In this paper, we adopt the two-dimensional engine structure to estimate the thrust [19], and it is shown in Figure 3.

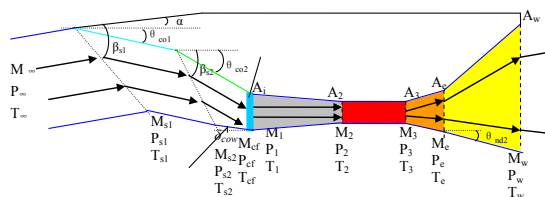


Fig. 3: Propulsive system configuration of hypersonic waverider.

According to Figure 3, the propulsive system configuration of hypersonic waverider consist of the first compression section, second compression section, diversion segment, airflow transition layer, engine inlet,

combustion chamber, first nozzle and second nozzle. Followed these, when the free flow passes through the lower surface in the first compression section, the oblique shock equation is used by [20]

$$\begin{cases} M_{s1} \sin(\beta_{s1} - \delta_1) = \sqrt{\frac{1 + \frac{\gamma_c - 1}{2} M_\infty^2 \sin^2 \beta_{s1}}{\gamma_c M_\infty^2 \sin^2 \beta_{s1} - \frac{\gamma_c - 1}{2}}} \\ P_{s1} = P_\infty \left[ 1 + \frac{2\gamma_c}{\gamma_c + 1} (M_\infty^2 \sin^2 \beta_{s1} - 1) \right] \\ T_{s1} = T_\infty \frac{P_{s1}}{P_\infty} \frac{2 + (\gamma_c - 1) M_\infty^2 \sin^2 \beta_{s1}}{(\gamma_c + 1) M_\infty^2 \sin^2 \beta_{s1}} \\ \tan(\delta_1) = \frac{2 \cot \beta_{s1} (M_\infty^2 \sin^2 \beta_{s1} - 1)}{M_\infty^2 (\gamma_c + 1 - 2 \sin^2 \beta_{s1}) + 2} \end{cases} \quad (9)$$

where  $\gamma_c$  is the gas constant, whereas  $M_{s1}, P_{s1}, T_{s1}$  are the compressed airflow parameters in the first compression section. Also, the calculation process of the second compression section is similar to the first part. Afterwards, the airstream enters into the diversion segment where the air mass flow rate is adjusted in line with the inlet cowl accordingly [21]. The resulting airstream state values are solved based on the isentropic equation of the variable area, and this is expressed by

$$\begin{cases} \frac{[1 + \frac{\gamma_c - 1}{2} M_{cf}^2]^{\frac{\gamma_c + 1}{\gamma_c - 1}}}{M_{cf}^2} = \left( \frac{A_{cf}}{A_{s2}} \right)^2 \frac{[1 + \frac{\gamma_c - 1}{2} M_{s2}^2]^{\frac{\gamma_c + 1}{\gamma_c - 1}}}{M_{s2}^2} \\ P_{cf} = P_{s2} \left[ \frac{1 + \frac{\gamma_c - 1}{2} M_{s2}^2}{1 + \frac{\gamma_c - 1}{2} M_{cf}^2} \right]^{\frac{\gamma_c}{\gamma_c - 1}} \\ T_{cf} = T_{s2} \left[ \frac{1 + \frac{\gamma_c - 1}{2} M_{s2}^2}{1 + \frac{\gamma_c - 1}{2} M_{cf}^2} \right] \\ \theta_{cf} = \tan \left( \frac{\tan \theta_{co2} + \tan \delta_{cowl}}{2} \right) \end{cases} \quad (10)$$

Followed that, the airflow state parameters in the airflow transition layer are decided by the oblique shock equation in Equation (9), but the airflow turning force appears in terms of the impulse theorem [22]. Once the airstream passes through this transition layer, its flow direction will parallel to the engine axis. We assume that the isentropic relation is satisfied at the inlet, so the computational procedure is same with Equation (10). After traversing this section, the airflow is mixed with the fuel in the combustion chamber, and then we have [22]

$$\begin{cases} \frac{M_3^2 (1 + \frac{\gamma_c - 1}{2} M_3^2)}{(1 + \gamma_c M_3^2)^2} = \frac{M_2^2 (1 + \frac{\gamma_c - 1}{2} M_2^2)}{(1 + \gamma_c M_2^2)^2} \\ + \frac{M_3^2}{(1 + \gamma_c M_2^2)^2} \frac{\Delta T}{T_2} \\ P_3 = P_2 \left[ \frac{1 + \gamma_c M_2^2}{1 + \gamma_c M_3^2} \right] \\ T_3 = T_2 \left[ \frac{1 + \gamma_c M_2^2}{1 + \gamma_c M_3^2} \right]^2 \left( \frac{M_3}{M_2} \right)^2 \\ \Delta T = \left[ \frac{f_{st} \phi}{1 + f_{st} \phi} \right] \left[ \frac{H_f \eta_c}{c_p} - \left( 1 + \frac{\gamma_c - 1}{2} M_2^2 \right) T_2 \right] \end{cases} \quad (11)$$

where  $f_{st}$  denotes the proper fuel-air ratio;  $\phi$  indicates the stoichiometric ratio;  $\eta_c$  represents the combustion efficiency;  $c_p$  is the heat capacity at constant pressure. Next, the airstream flows out of the combustion chamber

into the afterbody nozzle where the gas parameters are obtained according to Equation (10). Furthermore, the engine thrust are computed based on the momentum theorem [23], and this is written by

$$T = \dot{m}_a [V_1 - (1 + f) V_w] - (P_w - P_\infty) A_w - (P_1 - P_\infty) A_i \quad (12)$$

where  $f$  denotes fuel-air ratio, and  $\dot{m}_a$  is the air mass flow rate which is considered on condition that the second shock surface stands at the rear of the inlet cowl tip, as illustrated in Figure 4.

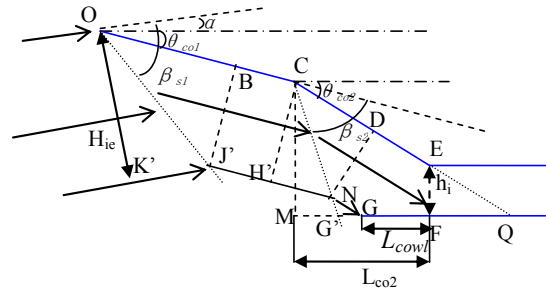


Fig. 4: Schematic diagram of second shock surface.

According to Figure 4, the equivalent height of the entering airflow is acquired by

$$\begin{aligned} H_{ie} &= |OK'| + |K'K| \\ &= \frac{|G'D| \sin \beta_{s2} \sin \beta_{s1}}{\sin(\beta_{s2} + \theta_{co1} - \theta_{co2}) \sin(\beta_{s2} - \alpha - \theta_{co1})} \\ &\quad + \frac{|GP| \sin \beta_{s1}}{\sin(\beta_{s1} - \alpha - \theta_{co1})} \\ &= \frac{(L_{co2} \tan \theta_{co2} + h_i) [\cot \theta_{co2} - \cot(\beta_{s2} + \theta_{co1})]}{\sin(\beta_{s2} + \theta_{co1} - \theta_{co2})} \\ &\quad \cdot \frac{\sin \theta_{co2} \sin \beta_{s2} \sin \beta_{s1}}{\sin(\beta_{s1} - \alpha - \theta_{co1})} \\ &\quad + \frac{[(L_{co2} \tan \theta_{co2} + h_i) \cot(\beta_{s2} + \theta_{co1}) + L_{nc1} - L_{co2}]}{\sin(\beta_{s1} - \alpha - \theta_{co1})} \cdot \sin \theta_{co1} \sin \beta_{s1} \end{aligned} \quad (13)$$

Therefore, the air mass flow rate without the sideslip angle is approximately determined by

$$\begin{cases} \dot{m}_a = P_\infty M_\infty A_{ie} \sqrt{\frac{\gamma_c}{RT_\infty}} \\ A_{ie} = H_{ie} W_{ni} \end{cases} \quad (14)$$

where  $W_{ni}$  is the forebody width. As soon as the aerodynamic force and the propulsive force are identified, the mathematical model of hypersonic morphing waverider is established as follows [24].

$$\begin{cases} \dot{V} = \frac{T \cos \alpha - D}{m} - \frac{\mu \sin \gamma}{(h + R_e)^2} \\ \dot{\gamma} = \frac{L + T \sin \alpha}{mV} - \frac{[\mu - V^2 (h + R_e)] \cos \gamma}{V(h + R_e)^2} \\ \dot{h} = V \sin \gamma \\ \dot{\alpha} = q - \dot{\gamma} \\ \dot{q} = M_y / I_y \end{cases} \quad (15)$$

where  $V, \alpha, h, q$  and  $\gamma$  indicate the velocity, angle of attack, altitude, pitch rate and flight path angle, respectively. These parameters make up of the flight states influenced by the morphing effect and control action in relation to the trim point and dynamic characteristics.

#### 4 Design methods of control integrated tool facing multidisciplinary analysis

According to Figure 2, the suitable control law needs to be designed to realize the multidisciplinary analysis, so the small perturbation linearization method is used to transfer the nonlinear model to the following linear model.

$$\begin{cases} \dot{x}_p = A_p x_p + B_p u \\ z_p = H_p x_p \end{cases} \quad (16)$$

where the state vector  $x_p = [\Delta V, \Delta \gamma, \Delta h, \Delta \alpha, \Delta q]^T$ ; the control input vector  $u = [\Delta \phi, \Delta \delta_e]^T$ ; the output vector  $z_p = [\Delta V, \Delta h]^T$ . And then we define the track error vector as

$$e_1 = r_d - H_p x_p \quad (17)$$

where the command signal vector  $r_d = [\Delta V_d, \Delta h_d]^T$ , and we let

$$x_2 = \int_0^t e_1(\tau) d\tau \quad (18)$$

In the combination of Equations (16) and (17), we have

$$\begin{pmatrix} \dot{x}_p \\ \dot{x}_2 \end{pmatrix} = Ax + Bu + Gr \quad (19)$$

$$= \begin{pmatrix} A_p & 0 \\ -H_p & 0 \end{pmatrix} \begin{pmatrix} x_p \\ x_2 \end{pmatrix} + \begin{pmatrix} B_p \\ 0 \end{pmatrix} u + \begin{pmatrix} 0 \\ I \end{pmatrix} r$$

Then, the error vector is redefined as the following form.

$$e = \begin{pmatrix} r - H_p x_p \\ x_2 \end{pmatrix} = \begin{pmatrix} I \\ 0 \end{pmatrix} r + \begin{pmatrix} -H_p & 0 \\ 0 & I \end{pmatrix} \begin{pmatrix} x_p \\ x_2 \end{pmatrix} \quad (20)$$

$$= Mr + Hx$$

At the same time, we select the quadratic performance index as

$$J = \frac{1}{2} \int_0^\infty (e^T Q e + u^T R u) dt \quad (21)$$

When substituting Equation (20) into Equation (21), we get

$$J = \frac{1}{2} \int_0^\infty (x^T H^T Q H x + 2r^T M^T Q H x + r^T M^T Q M r + u^T R u) dt \quad (22)$$

For the above equation, the according standard equation with respect to the Riccati and its adjoint vector are provided by

$$\begin{cases} \dot{P} = -PA - A^T P - H^T Q H + PBR^{-1}B^T P \\ \dot{g} = (PBR^{-1}B^T - A^T)g - (H^T Q M + P G)r \end{cases} \quad (23)$$

In Equation (23), there exists a unique positive definite solution  $P > 0$  such that the control law of the linear model in Equation (16) is obtained as the following form [25].

$$u = -K_x x - K_r r \quad (24)$$

where

$$\begin{cases} K_x = R^{-1}B^T P \\ K_r = (PBR^{-1}B^T - A^T)^{-1}(H^T Q M + P G) \end{cases} \quad (25)$$

According to the resulting control law, we further study the design issues of the multidisciplinary analysis tool, as demonstrated in Figure 5. The main functions of this tool need to involve the parametric modeling, aerodynamic and propulsive force calculation, dynamic characteristic analysis, control integrated iteration and so on.

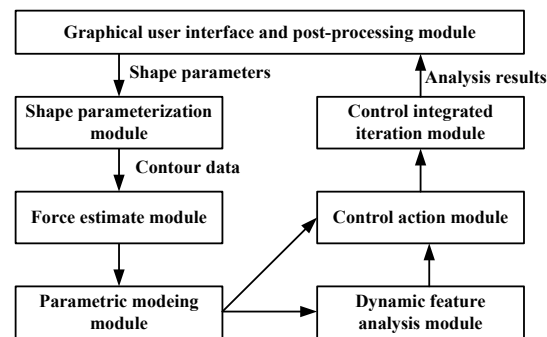


Fig. 5: Module diagram of Multidisciplinary analysis tool.

Figure 5 shows that the multidisciplinary analysis tool completes the shape parameterization for a given waverider configuration first, and then the relevant forces are estimated to construct the parametric model. Followed that, the dynamic characteristics are analyzed in terms of the task demands, and simultaneously the LQR control action are exerted. Afterwards, the integrated iteration is conducted combined with the control effect. Finally, the multidisciplinary analysis results are fed into the post-processing module, at the same time the shape parameters are re-adjusted in the graphical user interface accordingly. By the continuous iteration, the optimal shape parameters are determined for the given flight condition. Furthermore, the shape deformation regarding the different flight condition will depend on these optimal parameters so as to guarantee the matching relations between the morphing process and control action.

#### 5 Tool software development and simulation example

In this paper, the analysis tool of hypersonic morphing waverider is developed based on MATLAB and ANSYS.



First, we define the pivotal shape characteristic parameters, inputting them to the developed MATLAB GUI, and then provide the parameter constraints to compute the geometric structure. Afterwards, these shape parameters are brought in ANSYS wherein the waverider figure is acquired, and the following work is to deal with grid generation and to return them to MATLAB. Based on that, we further conduct the force estimation and model establishment in MATLAB wherein simultaneously accomplishing the control law design and control integrated iteration. Accordingly, the development course of the tool software is shown in Figure 6.

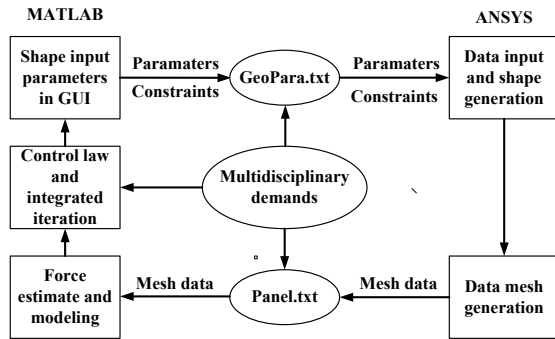


Fig. 6: Tool software development process.

In Figure 6, the tool software development process of hypersonic morphing waverider contains the following four steps:

- (1) The tool GUI is designed in MATLAB, and the waverider shape parameters are provided in relation to the corresponding computation conditions, as well the restrictions are calculated according to the real waverider structure. Moreover, the shape parameters and constrains are written into the file of GeoPara.txt.
- (2) The shape generation program is edited in ANSYS, and at the same time the shape parameters and constrains are inputted, leading to the waverider shape generation. Followed that, the mesh data of the waverider structure is obtained in line with the pre-defined rules.
- (3) The forces are estimated according to the loaded mesh data, and then the parametric model is established. At the same time, the dynamic features and trim states are gotten accordingly.
- (4) The control action is introduced into the parametric model such that the control integrated iteration can be accomplished based on the multidisciplinary demands. Whats more, the analysis results are feedbakced to the input interface, and also some post-processing work will be continued.

To illustrate the effectiveness of the proposed methods and built tool, a simulation example of hypersonic waverider is offered wherein the vehicle properties are

applied in Reference [22], so the developed analysis tool of hypersonic morphing waverider is demonstrated in Figure 7.

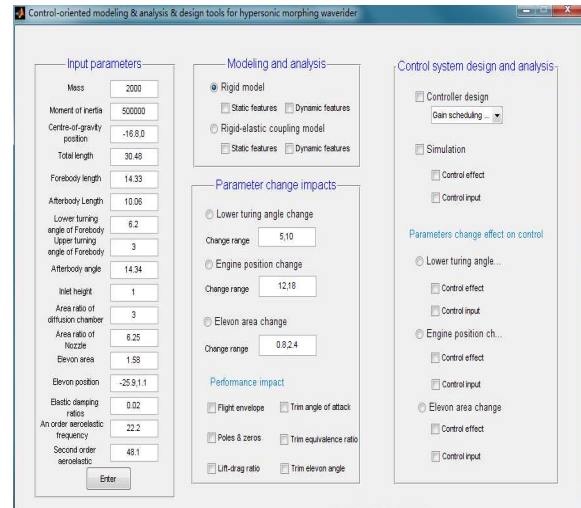


Fig. 7: Developed analysis tool of hypersonic morphing waverider.

According to Figure 7, we know the tool interface comprises four blocks: the shape parameter input, modelling and analysis, changing impact of the shape parameters and control integrated analysis. In fact, as long as the shape parameters are provided, the dynamic features and trim states can be obtained, and these results are provided in Figures 8 and 9.

	h=26 KM	h=25 KM	h=26 KM	h=27 KM	h=28 KM
M=7	0.8247	1.0443	1.2952	1.5812	1.9062
M=7.5	0.7982	0.9943	1.2190	1.4761	1.7692
M=8	0.7641	0.9408	1.1438	1.3764	1.6421
M=8.5	0.7277	0.8878	1.0719	1.2832	1.5249
M=9	0.6911	0.8367	1.0042	1.1967	1.4170

	h=26 KM	h=25 KM	h=26 KM	h=27 KM	h=28 KM
M=7	0.3485	0.2607	0.2760	0.2952	0.3192
M=7.5	0.2704	0.2626	0.2976	0.3163	0.3395
M=8	0.2957	0.3078	0.3225	0.3408	0.3632
M=8.5	0.3239	0.3358	0.3504	0.3682	0.3901
M=9	0.3547	0.3666	0.3810	0.3995	0.4198

	h=26 KM	h=25 KM	h=26 KM	h=27 KM	h=28 KM
M=7	11.9225	12.3039	12.7580	13.2991	13.9445
M=7.5	11.3234	11.6924	12.1244	12.6315	13.2279
M=8	10.8827	11.2314	11.6368	12.1091	12.6601
M=8.5	10.5479	10.8749	11.2538	11.6930	12.2028
M=9	10.2901	10.5960	10.9493	11.3578	11.8302

Fig. 8: Trim states of hypersonic morphing waveride.

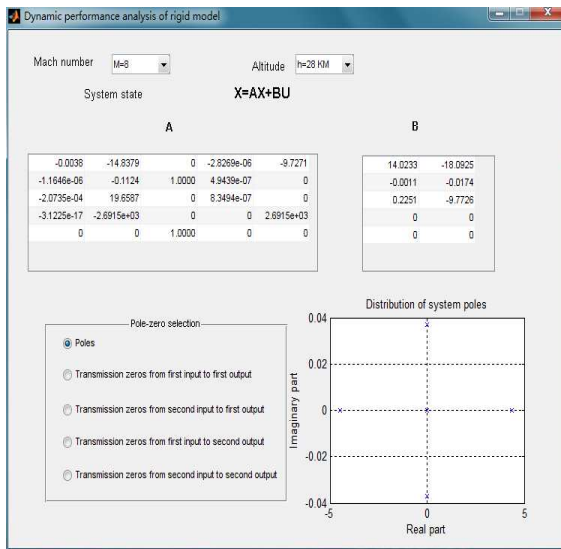


Fig. 9: Dynamic characteristics with regard to 8 Mach and 28km.

According to Figures 8 and 9, we find that the tool interface can provide facilities with the dynamic features analysis and equilibrium point contradistinction for the given flight velocity and altitude, and this makes the motion trends are intuitively compared when the flight conditions change. Furthermore, when considering the change of the shape parameters, the influences on the dynamic and static characteristics are demonstrated in Figures 10 and 11.

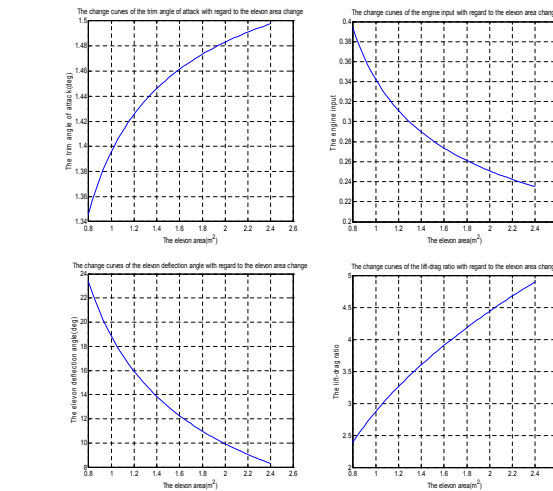


Fig. 11: Influence on trim states and lift-drag ratio with regard to eilon area change.

Figures 10 and 11 tell us that the trim states and lift-drag ratio change with the variations of the forebody turning angle and eilon area, which are relevant to the control action. This is because that the forebody turning angle change has the direct effect on the air mass flow rate, leading to the change of the propulsive force, whereas the eilon area decides the control efficiency. Therefore, the good control law needs to be designed to ensure the satisfied flight performance and to suppress the uncertain disturbances in the morphing process.

To further embody the coordinated relationship between the shape deformation and control quality, the subsequent results are obtained in the simulation interface, and they are provided in Figures 12 and 13.

According to Figures 12 and 13, we find that the system outputs ( $V$  and  $h$ ) can rapidly track the command signals ( $\Delta V_d = 100m/s$  and  $\Delta h_d = 100m/s$ ) from the trim point ( $V_0 = 2400m/s$  and  $h_0 = 27000m$ ) when the LQR control action is enforced. Nevertheless, the changes of the forebody tuning angle and eilon area play an important role in the control inputs and equilibrium states including the angle of attack, equivalence ratio and eilon deflection angle. In particular, these trim values are related with the flight performances, for example, the scramjet work well if the angle of attack can be limited within a certain range; whereas the eilon deflection angle is determined by the actuator ability intimately associated with the waverider weight and overall dimension. As a result, the appropriate compromise between the shape deformation and control action are helpful to improve the flight performance and control quality, thereby implementing the continuous waveriding flight.

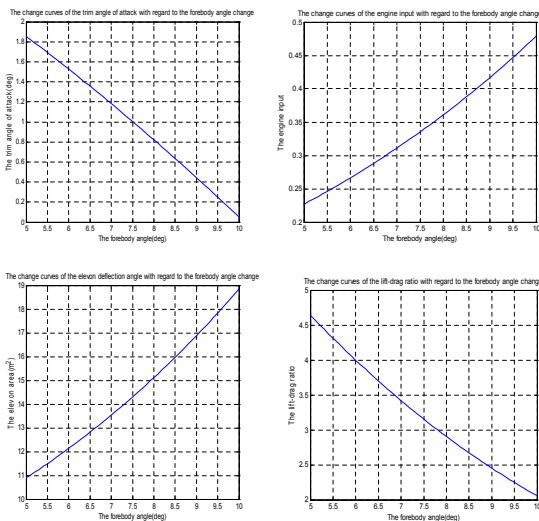
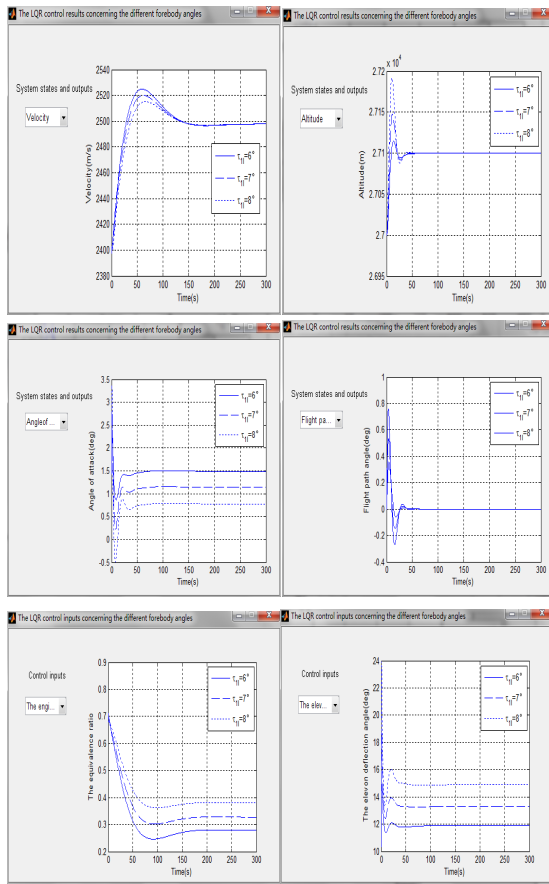


Fig. 10: Influence on trim states and lift-drag ratio with regard to forebody angle change.



**Fig. 12:** Response to command signals with regard to LQR control action and forebody tuning angle change.

## 6 Conclusion

In this paper, the multidisciplinary analysis tool based on the parametric model is discussed and developed for hypersonic morphing waverider. First, the implementation process is given to guide the following work. Next, the parametric model is established depending on the shape parameterization and force calculation by applying the quadratic curve methods and engineering estimation means. Afterwards, the control system is designed using the LQR control approaches, and the control action is introduced to the waverider model such that the control integrated design is realized based on the multidisciplinary analysis ideas. Finally, the development process of the tool software is proposed, and a simulation example is provided to illustrate the effectiveness of the presented methods. We believe this developed tool will be helpful to the further studies such as the control performance analysis and multidisciplinary optimization design.

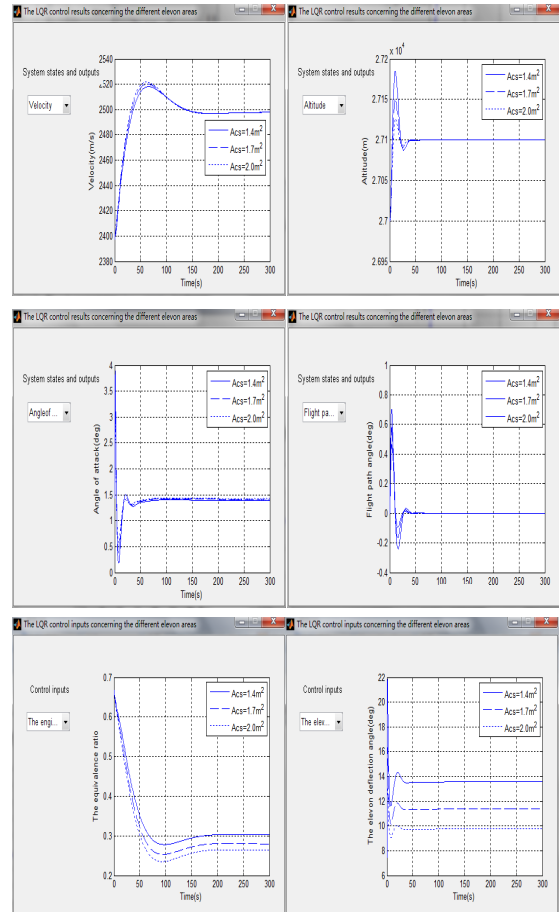


**Fig. 13:** Response to command signals with regard to LQR control action and elevon area change.

## Acknowledgement

This paper is supported by the NUAU Fundamental Research Funds under Grant no.NZ2013213.

## References

- [1] Xu, H.J, Ioannou, P.A and Mirmirani, M. Adaptive sliding mode control design for a hypersonic flight vehicle. *Journal of guidance, control and dynamics*, Vol. 27 No. 5, pp. 828-839, 2004.
- [2] Ahuja, V. and Hartfield, D. R. Optimization of air-breathing hypersonic aircraft design for maximum cruise speeds using genetic algorithms, In 16th AIAA/DLR/DGLR International Space Planes and Hypersonic Systems and Technologies Conference, Bremen, Germany, pp. 1-18, 2009.
- [3] Tsuchiya, T., Takenaka, Y. and Taguchi, H. Multidisciplinary design optimization for hypersonic experimental vehicle, *AIAA Journal*, Vol. 45 No. 7, pp. 1655-1662, 2007.
- [4] Yokoyama, N, Suzuki, S, Tsuchiya, T and et al. Multidisciplinary design optimization of space plane



- considering rigid body characteristics, *Journal of spacecraft and rockets*, Vol. 44 No. 1, pp. 122-131, 2007.
- [5] Rodriguez, A.A., Dickeson, J.J., Cifdaloz, O and et al. Modeling and control of scramjet-powered hypersonic vehicles: challenges, trends, & tradeoffs. In *AIAA guidance, navigation, and control conference and exhibit*, Honolulu, Hawaii, pp. 1-40, 2008.
- [6] Anderson, W. K., Karman, S. L. and Burdyslaw, C. Geometry Parameterization Method for Multidisciplinary Applications. *AIAA JOURNAL*, Vol.47, No.6, pp.1568-1578, 2009.
- [7] Hicken, J. E. and Zingg, D. W. Integrated geometry parameterization and grid movement using B-spline meshes. In *12th AIAA/ISSMO Multidisciplinary Analysis and Optimization Conference*, Victoria, British Columbia Canada, pp. 1-14, 2008.
- [8] Brenda, M. K. Universal Parametric Geometry Representation Method. *JOURNAL OF AIRCRAFT*, Vol.45, No.1, pp.142-158, 2008.
- [9] Frendreis, S. V. and Cesnik C. S. 3D Simulation of Flexible Hypersonic Vehicles. In *AIAA Atmospheric Flight Mechanics Conference*, Toronto, Ontario Canada, 2010.
- [10] Starkey, R. P. and Lewis, M. J. Simple Analytical Model for Parametric Studies of Hypersonic Waveriders. *Journal of Spacecraft and Rockets*, Vol. 36 No. 4, pp. 516-523, 1999.
- [11] Parker, J. H., Serran, A. and Yurkovich, S. Control-Oriented Modeling of an Air-Breathing Hypersonic Vehicle. *JOURNAL OF GUIDANCE, CONTROL, AND DYNAMICS*, Vol. 30 No.3, pp. 856-869, 2007.
- [12] Sun, H. F., Yang, Z. L. and Zeng, J. P. New Tracking-Control Strategy for Airbreathing Hypersonic Vehicles. *JOURNAL OF GUIDANCE, CONTROL, AND DYNAMICS*, Vol. 36 No.3, pp. 846-859, 2013.
- [13] Whitmer, C.E., Kelkar, A. G. and Vogel, J. M. Control Centric Parametric Trade Studies for Scramjet-Powered Hypersonic Vehicles. In *AIAA Guidance, Navigation, and Control Conference*, Toronto, Ontario Canada, pp. 1-29, 2010.
- [14] Soloway, D. I., Ouzts, P. J., Wolpert, D. H., et al. The Role of Guidance, Navigation, and Control in Hypersonic Vehicle Multidisciplinary Design and Optimization. In *16th AIAA/DLR/DGLR International Space Planes and Hypersonic Systems and Technologies Conference*, Moffett Field, CA, pp. 1-10, 2009.
- [15] Li, H. F., Lin, P. and Xu, D. J. Control-oriented Modeling for Air-breathing Hypersonic Vehicle Using Parameterized Configuration Approach. *Chinese Journal of Aeronautics*, Vol. 24 No.1, pp. 81-89, 2011.
- [16] Kelkar, A. G., Vogel, J. M., Whitmer, C. E., et al. Design Tool for Control-Centric Modeling, Analysis, and Trade Studies for Hypersonic Vehicles. In *17th AIAA International Space Planes and Hypersonic Systems and Technologies Conference*, San Francisco, California, pp. 1-33, 2011.
- [17] Oppenheimer, M. W., Doman, D. B. Hypersonic Vehicle Model Developed With Piston Theory. In *AIAA Atmospheric Flight Mechanics Conference and Exhibit*, Keystone, Colorado, pp. 1-20, 2006.
- [18] Dalle, D. J., Frendreis, S. V. and Driscoll, J. F et al. Hypersonic Vehicle Flight Dynamics with Coupled Aerodynamics and Reduced-order Propulsive Models. In *AIAA Atmospheric Flight Mechanics Conference*, Toronto, Ontario Canada, 2010.
- [19] Torrez, S. M., Driscoll, J. F. and Bolender, M. A. Effects of Improved Propulsion Modeling on the Flight Dynamics of Hypersonic Vehicles. In *AIAA Atmospheric Flight Mechanics Conference and Exhibit*, Honolulu, Hawaii, 2008.
- [20] Bolender, M.A., and Doman, D.B. A non-linear model for the longitudinal dynamics of a hypersonic air-breathing vehicle, In *AIAA Guidance, Navigation, and Control Conference and Exhibit*, San Francisco, California, pp. 1-22, 2005.
- [21] Kelkar, A. G., Vogel, J. M., and Inger, G. Modeling and Analysis Framework for Early Stage Trade-off Studies for Scramjet-Powered Hypersonic Vehicles. In *16th AIAA/DLR/DGLR International Space Planes and Hypersonic Systems and Technologies Conference*, Bremen, Germany, pp. 1-46, 2009.
- [22] Bolender, M. A. and Doman, D. B. Nonlinear longitudinal dynamical model of an air-breathing hypersonic vehicle, *Journal of spacecraft and rockets*, Vol. 44 No. 2, pp. 374-387, 2007.
- [23] Oppenheimer, M.W., Skujins, T., Doman, D. B. and et al. Canard-elevon interactions on a hypersonic vehicle, In *AIAA Atmospheric Flight Mechanics Conference and Exhibit*, Honolulu, Hawaii, pp. 1-13, 2008.
- [24] Liu, Y. B. and Lu, Y. P. Conceptual research on modeling and control integrative design methods for hypersonic waverider. *Proceedings of the Institution of Mechanical Engineers, Part G: Journal of Aerospace Engineering*, Vol. 225 No.12, pp.1291-1301, 2011.
- [25] Groves, K. P., Sigthorsson, D. O. and Serrani, A. Reference Command Tracking for a Linearized Model of an Air-breathing Hypersonic Vehicle, In *AIAA Guidance, Navigation, and Control Conference and Exhibit*, San Francisco, California, pp. 1-14, 2005.



**Yanbin Liu** received the Ph.D. degree from Nanjing University of Aeronautics and Astronautics, China, in 2007. He is a Associate Professor in College of Astronautics, Nanjing University of Aeronautics and Astronautics. His research interests include hypersonic flight control, modeling and control for the complex system.



**Liangqiang Zhou** received the Ph.D. degree in College of Aerospace Engineering from Nanjing University of Aeronautics and Astronautics, China, in 2008. He is a Associate Professor in College of Science, Nanjing University of Aeronautics and Astronautics. His research

interests include nonlinear mechanics, dynamical system and hypersonic dynamics.



**Yuping Lu** is a Professor in College of Astronautics, Nanjing University of Aeronautics and Astronautics. His research interests include advanced flight control, modeling and control for the complex system.